

DISPELLING ILLUSIONS OF REFLECTION: A NEW ANALYSIS OF THE 2007 MAY 19 CORONAL “WAVE” EVENT

GEMMA D. R. ATTRILL

Harvard-Smithsonian Center for Astrophysics, 60 Garden Street, Cambridge, MA 02138, USA
Received 2010 March 1; accepted 2010 May 24; published 2010 July 1

ABSTRACT

A new analysis of the 2007 May 19 coronal wave–coronal mass ejection–dimmings event is offered employing base difference extreme-ultraviolet (EUV) images. Previous work analyzing the coronal wave associated with this event concluded strongly in favor of purely an MHD wave interpretation for the expanding bright front. This conclusion was based to a significant extent on the identification of multiple reflections of the coronal wave front. The analysis presented here shows that the previously identified “reflections” are actually optical illusions and result from a misinterpretation of the running difference EUV data. The results of this new multiwavelength analysis indicate that two coronal wave fronts actually developed during the eruption. This new analysis has implications for our understanding of diffuse coronal waves and questions the validity of the analysis and conclusions reached in previous studies.

Key words: Sun: activity – Sun: corona – Sun: coronal mass ejections (CMEs) – Sun: UV radiation – Sun: X-rays, gamma rays

Online-only material: animations, color figures

1. INTRODUCTION

Coronal mass ejections (CMEs) are vast eruptions of magnetized plasma (typically 10^{15} – 10^{16} G) and magnetic flux (10^{20} – 10^{22} Mx) that explode from the solar atmosphere with velocities ranging from <100 to >3000 km s^{-1} (Gosling et al. 1976; Williams et al. 2005). Understanding the nascent stages of CMEs and their magnetic development as they expand is an active area of research. There are two low-coronal signatures of CMEs that are closely associated with their expansion, namely coronal dimmings and coronal waves. Coronal dimmings are primarily due to plasma evacuation during a significant expansion of the magnetic field, such as during a CME. Plasma outflows from coronal dimming regions have been measured most recently by the Extreme Ultraviolet Imaging Spectrometer on board *Hinode* (Culhane et al. 2007). Base difference (BD) images (where a pre-event frame is subtracted from all subsequent images) have traditionally been used to study coronal dimmings, though they also clearly show the earlier stages of coronal waves connected with dimming events. Coronal waves—also known colloquially as “EIT” waves after their discovery with the Extreme Imaging Telescope (EIT; Delaboudinière et al. 1995) on board the *Solar and Heliospheric Observatory (SOHO)*—are now also regularly observed by the Extreme Ultraviolet Imaging (EUVI; Wuelser et al. 2004) telescopes on board the *STEREO* spacecraft. Wills-Davey & Attrill (2010) review our changing understanding of coronal waves over the last solar cycle.

A consistent (and generally accepted) picture is emerging in the literature of two distinct types of coronal waves, based mainly on observed morphology (Vršnak 2005). In $\approx 7\%$ of EIT wave events, the bright front appears as a well-defined, sharp feature (Biesecker et al. 2002). These “brow waves” (Gopalswamy et al. 2000) or “S”-waves (Biesecker et al. 2002) often have high velocities ($>$ several hundred km s^{-1}), have a restricted arc-like angle of propagation, and are only (to my knowledge) ever observed near the initial source region. By far, however, the majority of EIT waves may be described as having a more diffuse bright front (e.g., Thompson et al. 1998, 1999;

Thompson & Myers 2009) and can be observed at distances from the source region on the scale of $1 R_{\odot}$. It is this latter diffuse bright front morphology that is observed during the 2007 May 19 event.

Historically, the most popular model for describing the characteristics of coronal waves is as a freely propagating fast-mode MHD wave/shock. Two key properties of fast-mode waves are that they travel at speeds $\geq v_A$ and can move perpendicular to the magnetic field. A recent summary of the main observational signatures that lend themselves to interpretation within the fast-mode description is given by Warmuth (2007). The reader is also referred to Attrill (2008, Section 3.5, and references therein). Since the minimum fast-mode speed is constrained by the Alfvén speed, any wave must travel faster than v_A for a fast-mode MHD solution to be valid. However, this is not the case for many coronal waves (Vršnak 2005; Wills-Davey et al. 2007; Zhukov et al. 2009). It has alternatively been suggested that slow-mode MHD waves (Krasnoselskikh & Podladchikova 2007), slow-mode shocks (and associated velocity vortices at the flank of the flux rope; see Wang et al. 2009), or solitary waves (Wills-Davey et al. 2007) may be responsible for generating the enhanced emission of the bright front. The current consensus is that diffuse coronal waves are CME-driven (e.g., Cliver et al. 2005) rather than being initiated by flares (e.g., Mann et al. 1999); see Vršnak & Cliver (2008) for a review. Indeed, Veronig et al. (2008) conclude that the 2007 May 19 event was driven by the CME expanding flanks, noting that the associated flare occurs too late to initiate the disturbance.

Conclusions in favor of a freely propagating fast-mode MHD wave model in studies such as those by Patsourakos et al. (2009) and Patsourakos & Vourlidis (2009) employ a cone model to fit the CME and so show that the CME base is distinct from the location of the diffuse coronal wave. However, such conclusions are forgone purely as a result of applying a fixed geometric model. Such an approach tells us nothing about the true CME expansion in the low corona. On the other hand, near-limb EUVI observations clearly show that CMEs can be significantly

distorted in the low corona, and attests that the diffuse coronal wave does, in fact, map the footprint of the CME throughout its (sometimes considerable $\approx R_{\odot}$) lateral expansion (for a clear example, see Attrill et al. 2009, their Figure 11). Case studies are building a growing body of evidence that the region below $1.3 R_{\odot}$ (i.e., below the *STEREO*/COR1 occulting disk) is the key to understanding the early stage development of CMEs. Sometimes near-limb EUV observations can fill this missing link; alternatively, sophisticated numerical simulations based on real magnetic field data can be used to study this region (e.g., Cohen et al. 2009). The results of these works require a revision of our understanding of CME origins away from the geometrically rigid cone model and toward a dynamic picture whereby the CME can expand to develop a footprint in the low corona with a diameter on the order of R_{\odot} .

It has also been suggested that diffuse coronal waves are not real waves at all. Rather, rearrangement of the magnetic structure during a CME may cause electric currents and compress the plasma at the boundaries between expanding stable flux domains, leading to the enhanced emission seen in coronal EUV lines (Delannée & Aulanier 1999; Delannée 2000, 2009; Chen et al. 2002, 2005a, 2005b; Chen 2009). In such a picture, stationary bright fronts are readily understood as being associated with separatrixes identifiable in the large-scale pre-eruptive magnetic field configuration. Delannée et al. (2008) found that a current shell is present during the dynamic phase of CME expansion, co-spatial with an enhanced density shell generated by plasma compression. This model requires line-of-sight integration over the altitude of the current shell to produce bright fronts. A significant Earthward-directed component to the expansion of a limb CME is required so that there is a substantial enough integration to progress the bright front across the disk, far from the limb. Whether this would be sufficient to generate coronal wave fronts that are consistent with observations of limb events (e.g., Attrill et al. 2007b; Cohen et al. 2009) remains to be demonstrated. Additionally, Delannée et al. (2008) note that the dissipation of the current densities at low altitude would not be responsible for the observed structure but that coronal waves are rather “high-altitude three-dimensional structures projected onto the solar disk.” In contrast, observations show that coronal wave fronts brighten plasma primarily within the lowest 1–2 scale heights (most recently shown by Patsourakos et al. 2009). A different model proposed by Attrill et al. (2007a) suggested that the diffuse coronal “wave” actually corresponds to the outermost flanks of the CME as it expands in the low corona, with the bright front itself the result of magnetic reconnections between the outermost shell of the CME and favorably oriented surrounding magnetic field. The coronal “wave” will naturally stop when the internal pressure is no longer large enough to drive reconnections with surrounding magnetic field (van Driel-Gesztelyi et al. 2008). Testing this concept in numerical simulations, Cohen et al. (2010) show evidence for reconnection between the expanding flux rope and neighboring closed loops, the result of which is to “step” the flux rope footpoint out of the original source region into the surrounding quiet Sun, thus expanding the CME footprint.

In support of the suggestion by Zhukov & Auchère (2004), Cohen et al. (2009) conclude that diffuse coronal waves consist of both a non-wave *and* a wave component. Specifically, they find that during the CME lateral expansion, the coronal wave maps the footprint of the CME, with the patchy, diffuse bright front due primarily to the compression of plasma (against both surrounding and overlying magnetic field). Some of the bright-

est concentrations correspond to the footpoints of reconnected magnetic field lines, and thus the non-wave component dominates. When the CME has expanded to its maximum lateral extent, the brightest parts of the coronal wave either disappear or become stationary before fading. What remains is a weaker, more uniform component that is consistent with an MHD wave interpretation. This weaker component exists throughout the expansion of the CME and continues to propagate even after the considerable CME lateral expansion has finished. In this later stage, the coronal wave is freely propagating, and is discernable in observations using the running difference (RD) processing method (where the previous image is subtracted from the current frame). RDs are particularly employed to follow the later-stage expansion of these events, which become increasingly difficult to detect in BD data.

2. PREVIOUS ANALYSES OF THE 2007 MAY 19 EVENT

Previous work analyzing the coronal wave associated with this event has concluded strongly in the favor of purely a wave interpretation, due largely to the identification of reflection. Specifically, Long et al. (2008): “. . .the disturbance shows strong reflection from a coronal hole,” Veronig et al. (2008): “. . .the wave was refracted and reflected at the coronal hole,” and Gopalswamy et al. (2009): “The wave reflection is clear evidence favoring the wave nature.” In particular, Gopalswamy et al. (2009) conclude that there are three reflections occurring in this event (see Figure 1): (1) northeast from the south polar coronal hole (CH), (2) eastward from the low-latitude CH located to the west of the solar disk, and (3) northward from the low-latitude CH.

All of these previous studies used RD images to analyze the coronal wave event. In this paper, I re-analyze the *STEREO*(B) EUVI data using BD images. I will show that previous works have analyzed artifacts present in RD images, rather than real brightenings and dimmings. Dramatically different results can be obtained by processing the data into RD or BD images (see, e.g., Chertok & Grechnev 2005). RD images emphasize *changes* of the brightness, location, and configuration of features occurring during the interval between two subsequent frames. However, they “distort the picture of large-scale disturbances caused by a CME” (Chertok & Grechnev 2005). In particular, real intensity decreases (coronal dimmings) and increases (such as the bright front of a coronal wave) can only be confidently identified and studied using BD images, and even then frequent reference to the original (non-differenced) data is important.

Schmidt & Ofman (2010) modeled the 2007 May 19 event with a three-dimensional time-dependent MHD code that includes real magnetogram data at the time of the coronal wave event and a solar wind outflow. They focus on the impact of a CME-driven shockwave on the surface, and study the resulting wave which spreads spherically over the solar surface. This wave has phase velocities in good agreement with theoretical values for a fast-mode magnetosonic wave. Schmidt & Ofman (2010) identify this wave with the diffuse bright front of the observed EUV coronal wave. Consistent with the previously published studies described above, they find that the incident wave is reflected at the boundary of the low-latitude CH (front 2, in Figure 1). They also conclude that the wave fronts that propagate to the north and south of the CH (fronts 1 and 3, in Figure 1) are due to resonant oscillation of the CH, which is excited by the incident wave.

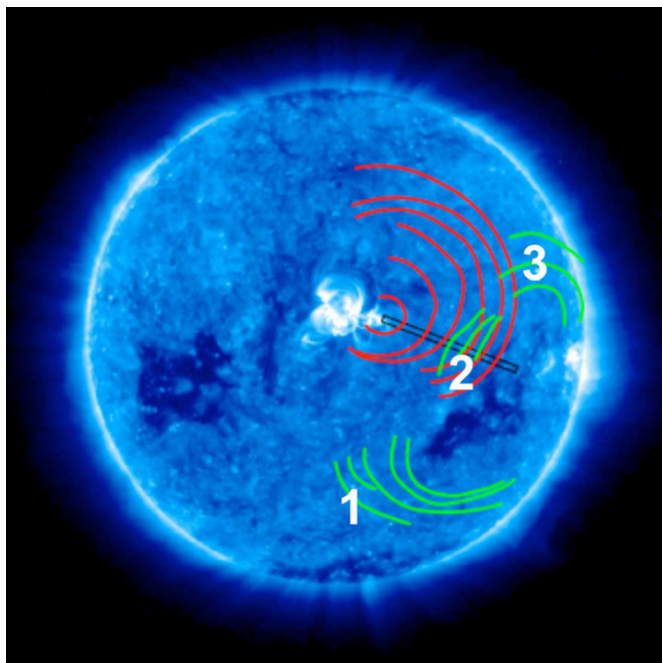


Figure 1. Figure adapted from Gopalswamy et al. (2009) showing the three reflections (green) of the incident coronal wave (red).

(A color version of this figure is available in the online journal.)

3. OBSERVATIONS

The eruption on 2007 May 19 at $\approx 12:40$ UT was associated with a double-CME event (at 13:24 and 13:48 UT) identified from the study of *SOHO*/LASCO C2 (Yashiro et al. 2004, http://cdaw.gsfc.nasa.gov/CME_list/), C3, and *STEREO*/COR1 data (Veronig et al. 2008; Möstl et al. 2009). I will argue here that there were also *two* coronal waves associated with this event, not just a single coronal wave, as considered in previous published works. I will show that one coronal wave expanded dominantly to the south of the active region (AR) exhibiting a clockwise rotation, while the second expanded northward. A magnetic cloud (MC) was observed in association with this event, and has been studied by Liu et al. (2008) and Möstl et al. (2009). Möstl et al. (2009) report that only the southern-directed CME can be associated with this MC. Both EUVI instruments observed this eruption; EUVI data from *STEREO*(B) are used here to analyze the coronal wave.

4. ANALYSIS

4.1. “Reflection 1”: From the South Polar Coronal Hole

Figure 2 (and Movie A of Figure 3) shows 195 Å RD images. (CHs are overlaid as contours in the movie. The movies accompanying the figures shown here are available in the electronic version of this paper.) The white arrows in Figure 2 highlight the front in Figure 5 of Gopalswamy et al. (2009), where they point to a brightening and follow it during successive frames. They conclude that the wave moving southward was reflected from the south polar CH, finally being stopped by the low-latitude CH to the (solar) east of the AR.

Figure 3 shows 195 Å RD images, with original intensity contours overlaid indicating the locations of the south polar and low-latitude CHs. The black arrows indicate the leading edge of the bright front that expands to the south of AR 10956. The white arrows highlight the location of the leading edge

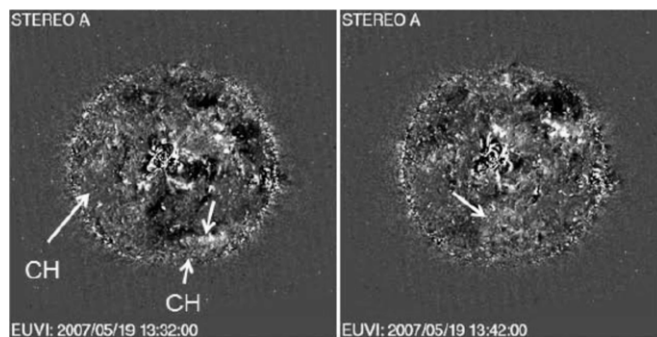


Figure 2. “Reflection” 1: figure from Gopalswamy et al. (2009), 195 Å RD images showing (left panel) the expansion of the coronal wave toward the south polar CH at 13:32 UT. The right panel at 13:42 UT shows the new location of the bright front (white arrow). Gopalswamy et al. (2009) conclude that the wave was reflected from the south polar CH.

bright front in the *previous* frame. The bright front only expands enough to directly encounter the south polar CH (which extends to $\approx -800''$ in the y -direction) between 13:42 and 13:52 UT (see the two movies associated with Figure 3). Therefore, it is erroneous to conclude that the bright front observed at 13:42 UT (right panel of Figure 2) is located at that position as a result of reflection from the south polar CH. Rather, by studying the evolution of the bright front before 13:32 UT (Figure 3), we find that the bright front *turns* clockwise during the expansion. The turning is underway by at least 13:12 UT.

Discovery of the rotation of diffuse coronal waves was made by Podladchikova & Berghmans (2005). Attrill et al. (2007a) independently confirmed this finding, additionally showing that individual diffuse coronal waves could exhibit a coherent rotation, the sense of which is dependent on the helicity of the CME source region. Specifically, coronal waves associated with a CME originating from a positive (negative) helicity source region were found to exhibit a clockwise (counterclockwise) rotation. Sigmoids are a well-known indicator of the magnetic helicity in a CME source region (Leamon et al. 2002), with a forward (reverse) “S” sigmoid indicating positive (negative) helicity. The source region of the 2007 May 19 CME (Figure 4) hosted a forward “S” positive helicity sigmoid. Thus, a clockwise rotation of the coronal wave (consistent with the observed turning evident in Figure 3) may actually be expected for this event.

Further evidence for the rotation of this coronal-wave–CME event can be found by examining the corresponding interplanetary data. Möstl et al. (2009) study an MC on 2007 May 22, and conclude that it is associated with the CME that expanded to the south of the AR. In this section, I analyze the coronal wave that expanded to the south of the AR, and I follow the understanding developed over the past three years that the coronal wave maps the footprint of the CME (Attrill et al. 2007a, 2007b; Attrill 2008). Möstl et al. (2009) report a difference of $\approx 110^\circ$ between the direction of the MC axial field at 1 AU and the axial field of the erupting plasmoid. They determine that the amount of rotation and its direction (clockwise) is consistent with the helical kink instability for a right-handed flux rope. Due to the faint nature of the coronagraph observation, Möstl et al. (2009) could not determine whether the rotation took place in the solar corona or farther out in the heliosphere. Due to the observed turning of the coronal wave from a dominantly southward toward an eastward direction (Figure 3), I suggest that the bright front indicates a clockwise rotation of $\approx 90^\circ$. Furthermore, it is possible to specify that this rotation is established between 13:12 and

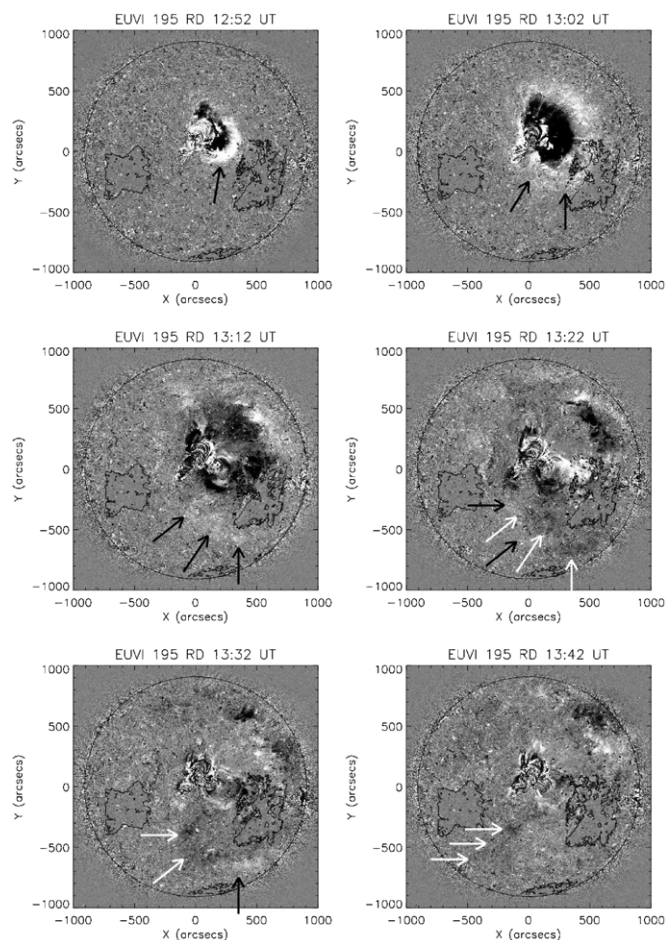


Figure 3. “Reflection 1”: 195 Å EUVI RD data with original intensity contours overlaid (black) indicating the location of the low-latitude and south polar CHs. The black arrows indicate the leading edge of the bright front that expands to the south of AR 10956. The white arrows highlight the location of the leading edge bright front in the *previous* frame. The bright front only actually reaches the south polar CH boundary between 13:42 and 13:52 UT (see Movie A and Movie B). Therefore, the front indicated by the white arrows in the right panel of Figure 2 at 13:42 UT cannot be the result of reflection from the south polar CH. Rather, the bright front *turns* clockwise during the expansion. The turning is underway by 13:12 UT.

(Animations of this figure are available in the online journal.)

13:42 UT during the early stages of the CME expansion in the low corona.

In summary, the coronal wave that expanded to the south of the AR was *not* reflected from the south polar CH as claimed by Gopalswamy et al. (2009). Rather, the coronal wave mapped the footprint of a CME that possessed positive helicity. The associated clockwise rotation was established during the early phase expansion of the CME, and this manifests in the EUVI observations as the rotation of the diffuse coronal wave in the low corona.

4.2. “Reflection 2”: to the East from the Low-latitude Coronal Hole

The “reflection” of the coronal wave front back toward the AR from the low-latitude CH (reflection 2 in Figure 1) was also identified in previous studies from the analysis of RD images. Figure 5 shows 171 Å RD and BD images of a zoomed-in area between the AR and western low-latitude CH, from 13:07 UT every 2 or 3 minutes until 13:19 UT. This time interval captures

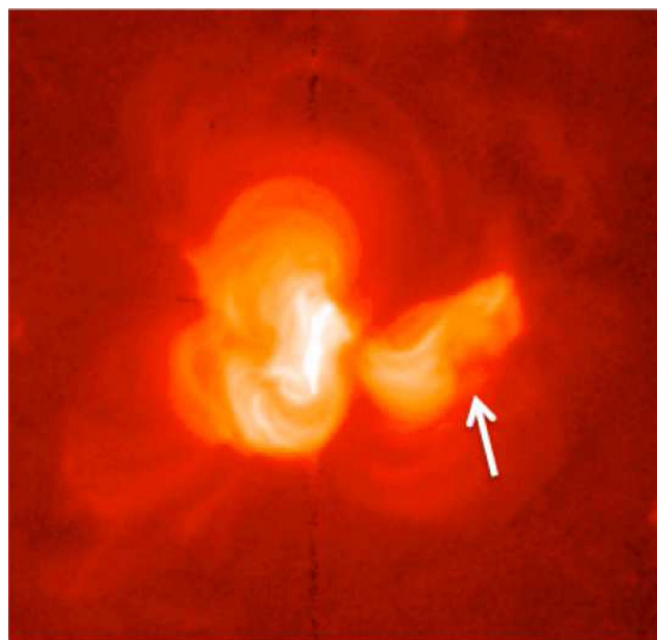


Figure 4. Pre-eruption *Hinode*/XRT synoptic image of NOAA AR 10956 at \approx 11:30 UT on 2007 May 19. The white arrow indicates the source region of the eruption. A forward “S” sigmoid structure can be identified.

(A color version of this figure is available in the online journal.)

the period during which “reflection 2” is underway (cf. Figure 2 in Gopalswamy et al. 2009). The reader is also encouraged to view the movies associated with Figure 5 (Movies A and B).

After the coronal wave reaches the low-latitude CH, the RD images in Figure 5 show brightenings (red arrows) that give the illusion of a reflection of the coronal wave from the low-latitude CH boundary back toward the AR. However, the corresponding BD images (yellow arrows) show that these brightenings are, in fact, artifacts created by the RD method. The RD brightenings indicate that a *change* has occurred between the current image and the previous one. They do *not* specify whether that change is an increase or a decrease in intensity. The BD images show that these changes (yellow arrows) are actually occurring in the coronal dimming regions that develop following the expansion of the coronal wave. I note that there is an exception to this finding: in the BD frame at 13:09 UT there are two orange arrows—these mark *real* brightenings present in the RD front.

Close examination of both the 171 and 195 Å BD movies (Figure 5 (Movie B) and Figure 3 (Movie B), respectively) shows that a limited part of the real bright front does, in fact, move significantly backward from the CH to the AR. This return brightening has a very localized nature (panels (c) and (d), Figure 6). From a previous study of the global magnetic environment associated with this sequence of eruptions in 2007 May, combined with the study of the original intensity data, this returning brightening can be attributed to compressed and heated plasma that is channeled along coronal loops, which are known to connect the eastern boundary of this low-latitude CH back to the AR (see Figure 7 in Attrill et al. 2009).

In summary, the bright front identified in the RD images that expanded to the west of the AR was *not* reflected from the eastern boundary of the low-latitude CH as claimed by Long et al. (2008), Veronig et al. (2008), and Gopalswamy et al. (2009). Their conclusions were essentially based on the analysis of an optical illusion, an artifact of the RD image processing.

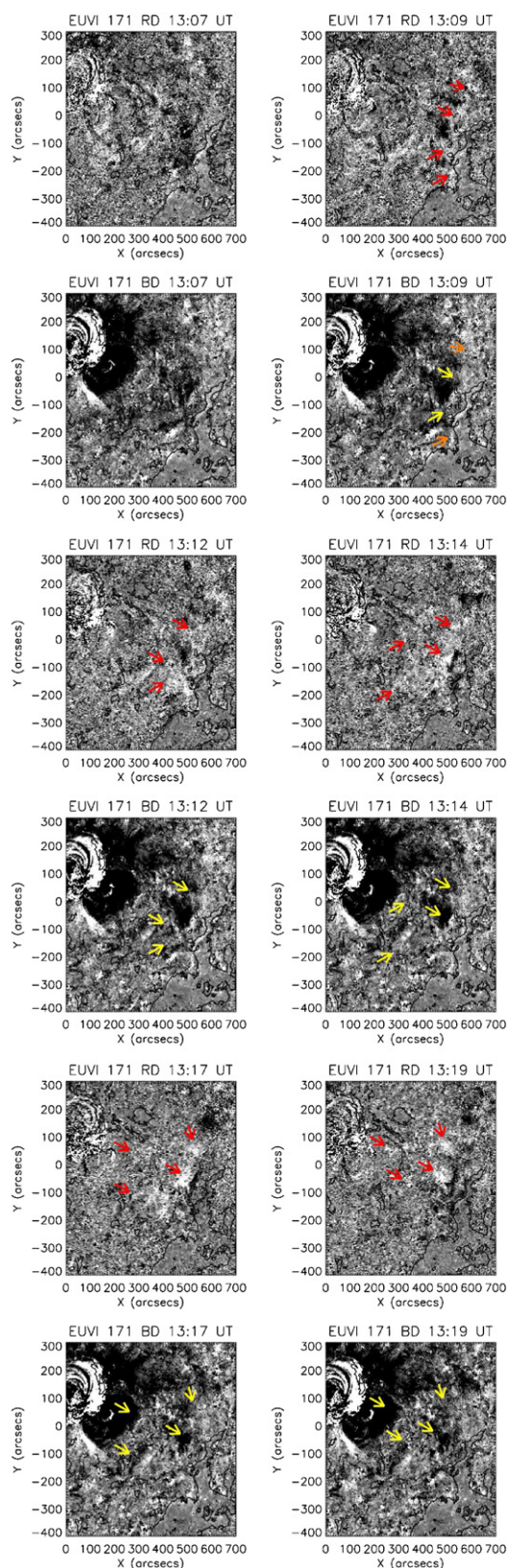


Figure 5. “Reflection” 2: 171 Å running (red arrows) and base (yellow arrows) difference images of the area between the AR and the western low-latitude CH (to the bottom right of each plot, outlined by a black contour). Red arrows highlight brightenings seen in the RD images, gradually moving away from the CH. Bottom panels of each section show BD images of the same area. Yellow arrows are drawn at the same locations as the red arrows. The two orange arrows in the BD frame at 13:09 UT indicate *real* brightenings.

(Animations of this figure (Movie A and Movie B) are available in the online journal.)

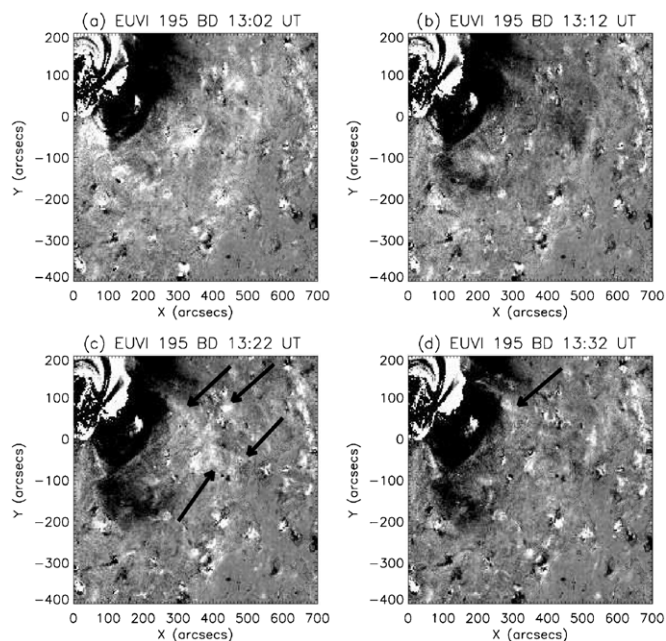


Figure 6. “Reflection” 2: 195 Å BD images, zoomed in to show the area between the AR and the western low-latitude CH (black contour). Panel (a) shows the incident coronal wave moving from the AR toward the CH. Panel (b) shows the dimming developing after the passage of the bright front. Panels (c) and (d) show a brightening (black arrows) moving *backward* from the CH toward the AR.

(An animation of this figure is available in the online journal.)

4.3. “Reflection 3”: to the North from the Low-latitude Coronal Hole

Gopalswamy et al. (2009) identify a third “reflection” of the coronal wave front, directed northward from the low-latitude CH (see Figure 1, reflection 3; Figure 7). In this section, I will show that the apparent behavior of the bright front to the north is also an illusion, a result of analyzing only RD images.

From the analysis of EUVI 171 Å and H α data, Veronig et al. (2008) report that two filaments erupt during this event. There is some ongoing discussion whether they actually merge or not (Veronig et al. 2008; Liewer et al. 2009; Bone et al. 2009). Regardless, the relevant point is that the eruption was composed of two parts—the southern part was associated with a neutral line within the AR, while the northern part extended as a quiescent filament into the quiet Sun (see Figure 8). Bone et al. (2009) concluded that both parts of the filament have positive magnetic helicity (consistent with the sense deduced from *Hinode*/XRT observations; see Figure 4). According to Bone et al. (2009), “the final eruption on May 19 proceeds in two parts, with initially the AR section of the filament erupting, followed by the quiescent section. . .”

The two-part nature of this eruption is implied in observations from other wavelengths as well. In Section 3, it was noted that a double-CME event was observed in white-light coronagraph data on 2007 May 19. The LASCO CME catalog records angular widths of 106° and 80° for the two CMEs, respectively. Although not one-to-one, it is known that there is a strong statistical relationship between CMEs and coronal waves (Biesecker et al. 2002), and it has been demonstrated that CMEs with large angular widths tend to have associated coronal waves (Attrill 2008). In such cases, the coronal wave maps the footprint of the associated CME (Thompson et al. 1999; Attrill et al. 2007b,

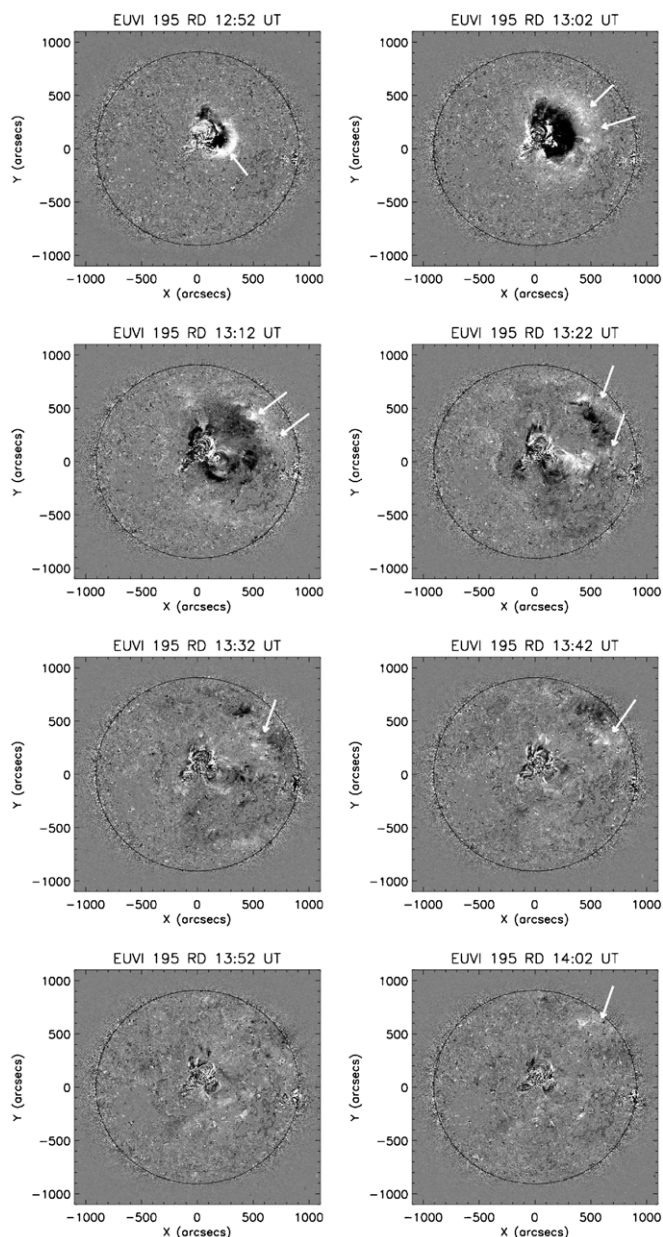


Figure 7. “Reflection” 3: RD 195 Å images. The white arrows indicate the “reflection” northward from the low-latitude CH (black contour) that is referred to in previous studies of this event.

(An animation of this figure is available in the online journal.)

2009; Cohen et al. 2009; Dai et al. 2010). Analysis of the EUVI BD data confirms that there are actually *two* coronal wave fronts associated with the 2007 May 19 double-CME event.

Figure 9 shows 195 Å BD EUVI images during the first 20 minutes of the event. The bright front associated with the AR part of the filament eruption expands first (white arrows in Figure 9), consistent with the H α observations. The expansion is predominantly to the south and west. The AR-associated coronal wave bright front reaches the west limb first. The quiescent filament part of the eruption occurs slightly later and drives the bright front predominantly to the north and west (black arrows in Figure 9). The slight delay between the initiation of the AR and quiescent parts of the filament eruption means that in the northwest quadrant, the expansion of the AR bright front to the west is followed slightly later by the quiescent-driven bright

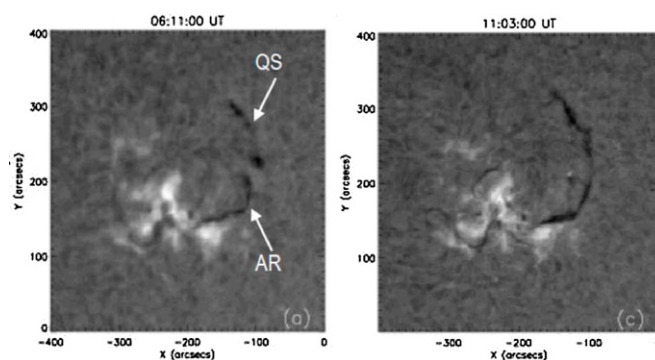


Figure 8. H α filament observations from the Kanzelhöhe Solar Observatory at 06:11 and 11:03 UT on 2007 May 18. “AR” and “QS” indicate the parts of the filament associated with the active region and quiescent Sun, respectively. (Figures reproduced courtesy of Bone et al. 2009.)

front, directed to the northwest. In the RD images, this amounts to a *perceived* change in the direction of the bright front from a westerly to a northerly direction (white arrows in Figure 7). Due to the proximity to the low-latitude CH to the west of the AR, this has previously been incorrectly attributed to a reflection of the front from the CH. However, the bright fronts visible in the BD data (Figure 9) can be straightforwardly attributed to the closely coupled eruptions—the first one dominantly to the southwest and the second dominantly to the northwest.

This understanding allows us to resolve a difficulty encountered by Gopalswamy et al. (2009) who report that “the reflected wave north has a speed higher than that of the direct wave.” With this new analysis of the real intensity changes, it is now apparent that the front that moves to the north (their “reflected wave”) is actually driven by a different (later) part of the filament eruption than the part that expands to the west (their “incident wave”). In summary, the BD EUVI data show that there is actually no change in direction or reflection in the northwest quadrant, but rather the arrival of two separate coronal wave fronts that are driven in different directions. Therefore, “reflection” 3, as for “reflections” 1 and 2, amounts to no more than an optical illusion.

5. DISCUSSION

This case study highlights the importance of using BD and not solely RD images for even a cursory analysis of coronal wave and dimming events. RD images are undoubtedly useful for highlighting subtle changes between frames and for drawing the eye toward moving fronts. However, it is crucial that this information be interpreted correctly, and it must be understood that brightenings and dimmings in RD data do *not* indicate real intensity changes. This is fundamental to establish before any conclusions can be drawn from the data analysis. Chertok & Grechnev (2005) detail the differences between using RDs and BDs for the analysis of the famous 2000 July 14 Bastille Day event.

When using difference images, the observer must always beware of optical illusions and exercise care in determining what they are actually looking at. Even when using BD images, when observing a brightening during a coronal wave event, basic questions such as “Is it really a coronal wave front?” must still be considered. As Attrill et al. (2009) showed, brightenings in BD data that initially appear to be components of a coronal wave can instead be due to plasma compression and the channeling

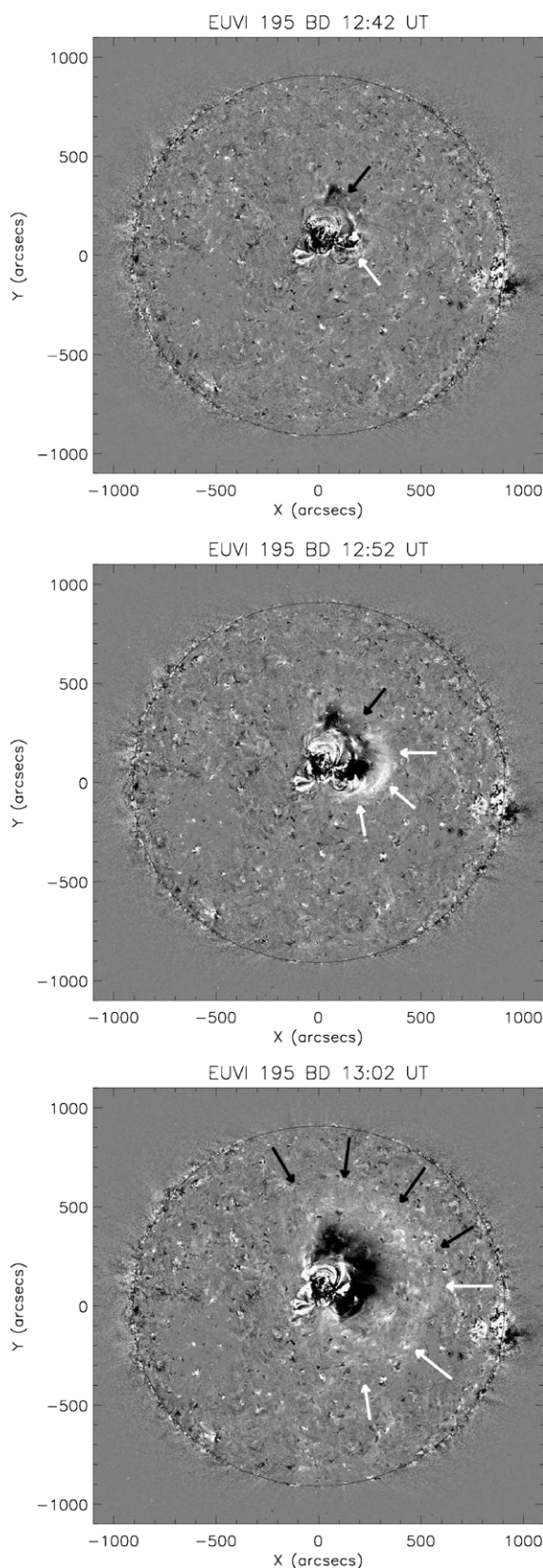


Figure 9. “Reflection” 3: 195 Å BD data with arrows highlighting the two distinct coronal wave fronts. The front indicated by the white arrows is associated with the AR part of the filament eruption, and starts first. In these early frames of the event, the expansion is dominantly to the south and west. This is closely followed by the quiescent (QS) part of the filament eruption, which drives the bright front indicated by black arrows. This expansion is dominantly toward the north and west.

(An animation of this figure is available in the online journal.)

of the heated plasma along large-scale coronal loops. As Delannée & Aulanier (1999) first proposed, the influence of the global-scale magnetic field is of fundamental importance and must be considered when analyzing coronal wave events.

The analysis presented here has shown that the behavior of the 2007 May 19 coronal waves can be understood without invoking reflection. Rather, the interplay (coupled nature) of brightenings and dimmings is emphasized in this analysis. I challenge the conclusions previously reached identifying far-reaching “reflections” of the coronal wave front during this event. I seriously question the evidence that these studies offered in support of MHD wave theories, since these conclusions are essentially based upon the analysis of optical illusions.

In the numerical simulation work by Schmidt & Ofman (2010), the potential relationship of the reflected wave (resulting from a CME-driven shockwave impacting the solar surface) to the diffuse bright front in EUV observations might be re-evaluated in the context of the new analysis presented here. I would like to emphasize that this new analysis does not exclude the generation of a real wave component (indeed, see Cohen et al. 2009), rather, it simply shows that the diffuse bright fronts observed in EUV data do not exhibit far-reaching reflection from the surrounding CHs, as previously claimed. Indeed the *lack* of such reflections in this event, despite the abundance of surrounding CHs, rather begs the question: if the diffuse bright fronts during the expansion stage of the CME are actually waves, then why *do we fail* to observe any reflection? The lack of reflection actually constitutes further evidence against a freely propagating interpretation for coronal waves. As shown repeatedly in multiple analyses (e.g., Attrill et al. 2007b, 2009; Chen 2009; Cohen et al. 2009; Dai et al. 2010), the coronal wave bright front is directly driven by the low coronal, lateral expansion of the CME, and maps the CME footprint in the low corona. Therefore, a priori, it *cannot* undergo a direct far-reaching reflection. This can be understood using the snow-plough analogy—the coronal wave cannot reflect back to the source region while the CME continues to expand laterally.

Based on their analysis, Gopalswamy et al. (2009) state that the reflection of coronal waves from CHs is “quite common.” Having demonstrated here that the “reflections” previously identified in the 2007 May 19 event are, in fact, optical illusions, I would like to clarify that the reflection of coronal waves from CHs is actually a most elusive observation. In contrast, coronal waves are observed to either become stationary or disappear at CH boundaries (e.g., Thompson et al. 1998; Attrill et al. 2006, 2007b; Veronig et al. 2006).

Finally, a comment concerning the direct mapping of the coronal wave to the CME footprint in the low corona. Diffuse coronal waves show us the extent of the CME lateral expansion in the low corona. The much-employed cone models for CMEs *cannot* be applied to CMEs that are associated with coronal waves for studying their development in the low corona. At the very least, the point of the conic section must be cut off so that the intersection with the low corona covers a much larger area. In some cases, even this adjustment is insufficient—near-limb event case studies have shown that the behavior of the CME in the low corona (below $\approx 1.3 R_{\odot}$) can be strongly non-radial (see Attrill et al. 2009, their Figure 11, for an example). CMEs are complex magnetic eruptions that evolve dramatically as they interact and reconnect with the ambient magnetic field that they encounter during their expansion. The future study of CME evolution should focus on this interaction (e.g., Soenen et al. 2009; Cohen et al. 2009, 2010) and progress away from

the study of CMEs as isolated entities. In order to advance our understanding of the early stage evolution of CMEs and their associated low coronal signatures, the research community must adapt long-held assumptions of dominantly radial expansion and idealistic geometric constraints.

6. CONCLUSIONS

A new analysis of the 2007 May 19 coronal wave–CME–dimmings event using BD EUV images is presented. The results indicate that there were actually two coronal wave fronts present during the eruption, which were likely associated with the two-part filament eruption and double-CME that accompanied this event. The coronal wave that expanded to the south exhibited a significant clockwise rotation, consistent with the CME originating from a positive helicity source region as well as the orientation of the associated MC.

Previous work analyzing the coronal wave associated with this event concluded strongly in favor of purely a wave interpretation for the expanding bright front (Long et al. 2008; Veronig et al. 2008; Gopalswamy et al. 2009). This conclusion was based to a significant extent on the identification of multiple reflections of the coronal wave front. This paper demonstrates that the conclusions of these previous studies are seriously questionable, since they are essentially based upon the analysis of optical illusions created by an incorrect analysis of RD EUV data.

I appreciate the helpful comments from the referee which clarified this work. I would also like to sincerely thank N. Gopalswamy, A. Veronig, and P. Gallagher for discussions concerning the analysis of this complex event. I am extremely grateful to L. van Driel-Gesztelyi, P. Démoulin, L. Culhane, L. Harra, O. Cohen, N. Nitta, A. Engell, M. Wills-Davey, and the SXXG group at SAO for discussion developing various aspects of this work. My thanks also to C. Möstl for initiating discussion regarding the interplanetary component of this CME event, and the connection with the low coronal counterpart. The *STEREO*/SECCHI data are produced by an international consortium: NRL, LMSAL, NASA, GSFC (USA); RAL (UK); MPS (Germany); CSL (Belgium); and IOTA, IAS (France). *SOHO* is a project of international cooperation between ESA and NASA. This research has made use of NASA's Astrophysics Data System Bibliographic Services. I acknowledge NASA grant NNX09AB11G which supported this work.

REFERENCES

- Attrill, G. D. R. 2008, PhD thesis, Univ. College London
- Attrill, G. D. R., Engell, A. J., Wills-Davey, M. J., Grigis, P., & Testa, P. 2009, *ApJ*, **704**, 1296
- Attrill, G. D. R., Harra, L. K., van Driel-Gesztelyi, L., & Démoulin, P. 2007a, *ApJ*, **656**, L101
- Attrill, G. D. R., Harra, L. K., van Driel-Gesztelyi, L., Démoulin, P., & Wülser, J.-P. 2007b, *Astron. Nachr.*, **328**, 760
- Biesecker, D. A., Myers, D. C., Thompson, B. J., Hammer, D. M., & Vourlidas, A. 2002, *ApJ*, **569**, 1009
- Bone, L. A., van Driel-Gesztelyi, L., Culhane, J. L., Aulanier, G., & Liewer, P. 2009, *Sol. Phys.*, **259**, 31
- Chen, P. F. 2009, *ApJ*, **698**, L112
- Chen, P. F., Ding, M. D., & Fang, C. 2005a, *Space Sci. Rev.*, **121**, 201
- Chen, P. F., Fang, C., & Shibata, K. 2005b, *ApJ*, **622**, 1202
- Chen, P. F., Wu, S. T., Shibata, K., & Fang, C. 2002, *ApJ*, **572**, L99
- Chertok, I. M., & Grechnev, V. V. 2005, *Sol. Phys.*, **229**, 95
- Cliver, E. W., Laurenza, M., Storini, M., & Thompson, B. J. 2005, *ApJ*, **631**, 604
- Cohen, O., Attrill, G. D. R., Manchester, W. B., & Wills-Davey, M. J. 2009, *ApJ*, **705**, 587
- Cohen, O., Attrill, G. D. R., Schwadron, N. A., Crooker, N. U., Owens, M. J., Downs, D., & Gombosi, T. I. 2010, *J. Geophys. Res.*, submitted
- Culhane, J. L., et al. 2007, *Sol. Phys.*, **243**, 19
- Dai, Y., Auchère, F., Vial, J. C., Tang, Y. H., & Zong, W. G. 2010, *ApJ*, **708**, 913
- Delaboudinière, J.-P., et al. 1995, *Sol. Phys.*, **162**, 291
- Delannée, C. 2000, *ApJ*, **545**, 512
- Delannée, C. 2009, *A&A*, **495**, 571
- Delannée, C., & Aulanier, G. 1999, *Sol. Phys.*, **190**, 107
- Delannée, C., Török, T., Aulanier, G., & Hochedez, J.-F. 2008, *Sol. Phys.*, **247**, 123
- Gopalswamy, N., Kaiser, M. L., Sato, J., & Pick, M. 2000, in ASP Conf. Ser. 206, High Energy Solar Physics Workshop—Anticipating Hessi, ed. R. Ramaty & N. Mandzhavidze (San Francisco, CA: ASP), 351
- Gopalswamy, N., et al. 2009, *ApJ*, **691**, L123
- Gosling, J. T., Hildner, E., MacQueen, R. M., Munro, R. H., Poland, A. I., & Ross, C. L. 1976, *Sol. Phys.*, **48**, 389
- Krasnoselskikh, V., & Podladchikova, O. 2007, AGU Fall Meeting Abstracts, A1047
- Leamon, R. J., Canfield, R. C., & Pevtsov, A. A. 2002, *J. Geophys. Res.*, **107**, 1234
- Liewer, P. C., de Jong, E. M., Hall, J. R., Howard, R. A., Thompson, W. T., Culhane, J. L., Bone, L., & van Driel-Gesztelyi, L. 2009, *Sol. Phys.*, **256**, 57
- Liu, Y., Luhmann, J. G., Huttunen, K. E. J., Lin, R. P., Bale, S. D., Russell, C. T., & Galvin, A. B. 2008, *ApJ*, **677**, L133
- Long, D. M., Gallagher, P. T., McAteer, R. T. J., & Bloomfield, D. S. 2008, *ApJ*, **680**, L81
- Mann, G., Klassen, A., Estel, C., & Thompson, B. J. 1999, in 8th *SOHO* Workshop: Plasma Dynamics and Diagnostics in the Solar Transition Region and Corona, ed. J.-C. Vial & B. Kaldeich-Schü (ESA SP-446; Noordwijk: ESA), 477
- Möstl, C., et al. 2009, *J. Geophys. Res.*, **114**, A04102
- Patsourakos, S., & Vourlidas, A. 2009, *ApJ*, **700**, L182
- Patsourakos, S., Vourlidas, A., Wang, Y. M., Stenborg, G., & Thernisien, A. 2009, *Sol. Phys.*, **259**, 49
- Podladchikova, O., & Berghmans, D. 2005, *Sol. Phys.*, **228**, 265
- Schmidt, J. M., & Ofman, L. 2010, *ApJ*, submitted
- Soenen, A., Bemporad, A., Jacobs, C., & Poedts, S. 2009, *Ann. Geophys.*, **27**, 3941
- Thompson, B. J., & Myers, D. C. 2009, *ApJS*, **183**, 225
- Thompson, B. J., Plunkett, S. P., Gurman, J. B., Newmark, J. S., St. Cyr, O. C., & Michels, D. J. 1998, *Geophys. Res. Lett.*, **25**, 2465
- Thompson, B. J., et al. 1999, *ApJ*, **517**, L151
- van Driel-Gesztelyi, L., Attrill, G. D. R., Démoulin, P., Mandrini, C. H., & Harra, L. K. 2008, *Ann. Geophys.*, **26**, 3077
- Veronig, A. M., Temmer, M., & Vršnak, B. 2008, *ApJ*, **681**, L113
- Veronig, A. M., Temmer, M., Vršnak, B., & Thalmann, J. K. 2006, *ApJ*, **647**, 1466
- Vršnak, B. 2005, *EOS Trans. Am. Geophys. Union*, **86**, 112
- Vršnak, B., & Cliver, E. W. 2008, *Sol. Phys.*, **253**, 215
- Wang, H., Shen, C., & Lin, J. 2009, *ApJ*, **700**, 1716
- Warmuth, A. 2007, in Lect. Notes in Phys. 725, The High Energy Solar Corona: Waves, Eruptions, Particles, ed. K.-L. Klein & A. L. MacKinnon (Berlin: Springer), 107
- Williams, D. R., Török, T., Démoulin, P., van Driel-Gesztelyi, L., & Kliem, B. 2005, *ApJ*, **628**, L163
- Wills-Davey, M. J., & Attrill, G. D. R. 2010, *Space Sci. Rev.*, **22**
- Wills-Davey, M. J., DeForest, C. E., & Stenflo, J. O. 2007, *ApJ*, **664**, 556
- Wuelser, J.-P., et al. 2004, Proc. SPIE, **5171**, 111
- Yashiro, S., Gopalswamy, N., Michalek, G., St. Cyr, O. C., Plunkett, S. P., Rich, N. B., & Howard, R. A. 2004, *J. Geophys. Res.*, **109**, 7105
- Zhukov, A. N., & Auchère, F. 2004, *A&A*, **427**, 705
- Zhukov, A. N., Rodriguez, L., & de Patoul, J. 2009, *Sol. Phys.*, **259**, 73